Mathematical modelling suggests differential impact of {beta}-TrCP paralogues on Wnt/{beta}-catenin signalling dynamics

Benary, U., Kofahl, B., Hecht, A., Wolf, J.

Mathematical Modelling suggests Differential Impact of β-TrCP Paralogues on Wnt/ β-catenin Signalling Dynamics

Uwe Benary [1]; Bente Kofahl [1]; Andreas Hecht [2]; Jana Wolf [1]

[1] Mathematical Modelling of Cellular Processes, Max Delbrück Center for Molecular Medicine Berlin-Buch, Berlin, Germany
[2] Institute of Molecular Medicine and Cell Research and BIOSS Centre for Biological Signalling Studies, Albert-Ludwigs-Universität Freiburg, Freiburg, Germany

Corresponding author:

Dr. Jana Wolf

Mathematical Modelling of Cellular Processes

Max Delbrück Center for Molecular Medicine (MDC), Berlin-Buch

Robert-Rössle-Str. 10

13125 Berlin

Germany

Fax: +49 30 9406 2394

Tel.: +49 30 9406 2641

E-Mail: jana.wolf@mdc-berlin.de

URL of website: www.mdc-berlin.de

Article type : Original Article

Running title: Impact of β-TrCP on Wnt/ β-catenin Dynamics.

Abbreviations: APC, adenomatous polyposis coli protein; Axin, axis inhibition protein; CK1, casein kinase 1; CRD-BP, coding region determinant-binding protein; Dkk, Dickkopf; Dsh, Dishevelled; FWD1, F-box/WD repeat-containing protein 1A (also known as ẞ-TrCP1); GSK3, glycogen synthase kinase 3; HOS, Homologous to Slimb protein (also known as ẞ-TrCP2); I κB, inhibitor of nuclear factor κ-light-chain-enhancer of activated B cells (NF-kB); JNK, c-Jun N-terminal kinase; LRP5/6, low-density lipoprotein (LDL) receptor-related protein 5/6; MAPK, mitogen-activated protein kinases; Mdm2, Mouse double minute 2 homolog; ODE, ordinary differential equation; PKB, Protein Kinase B; SCF, S-phase kinase-associated protein (Skp)-Cullin-F-box complex; siRNA, small interfering RNA; TBEs, TCF

binding elements; TCF, T-cell factor/lymphoid enhancer factor (LEF) family; β-TrCP, β-transducin repeat-containing protein

Keywords: HOS, FWD1, feedback, APC mutation, cancer

1. Abstract

The Wnt/β-catenin signalling pathway is involved in the regulation of a multitude of cellular processes by controlling the concentration of the transcriptional regulator β-catenin. Proteasomal degradation of β-catenin is mediated by the two β-transducin repeat-containing protein (β-TrCP) paralogues HOS and FWD1, which are functionally interchangeable and thereby considered to function redundantly in the pathway. HOS and FWD1 are both regulated by Wnt/β-catenin signalling, albeit in opposite directions, thus establishing interlocked negative and positive feedback loops. The functional relevance of the opposite regulation of HOS and FWD1 by Wnt/β-catenin signalling in conjunction with their redundant activities in proteasomal degradation of β-catenin is an unresolved issue. Using a detailed ordinary differential equation (ODE) model, we investigated the specific influence of each individual feedback mechanism and their combination on Wnt/β-catenin signal transduction under wild type and cancerous conditions. We found that under wild type conditions the signalling dynamics are predominantly affected by the HOS feedback due to a higher concentration of HOS than FWD1. Transcriptional up-regulation of FWD1 by other signalling pathways reduced the impact of the HOS feedback. The opposite regulation of HOS and FWD1 expression by Wnt/β-catenin signalling allows employing the FWD1 feedback as a compensation mechanism against aberrant pathway activation due to reduced HOS concentration. In contrast, the FWD1 feedback provides no protection against aberrant activation in APC mutant cancer cells.

2. Introduction

The Wnt/β-catenin signalling pathway plays central roles in many key cellular processes such as cell proliferation and differentiation, mainly by exerting tight control on gene expression [1-3]. To achieve this, Wnt/β-catenin signalling needs to effectively regulate the concentration and the activity of the transcriptional regulator β-catenin [4, 5]. In resting cells, the concentration of unbound β-catenin remains low because its permanent production is counterbalanced by its continuous degradation. The degradation is primarily mediated by a

destruction complex [6]. In this complex, axis inhibition protein (Axin) and adenomatous polyposis coli protein (APC) form a scaffold that allows casein kinase 1 (CK1) and glycogen synthase kinase 3 (GSK3) to sequentially phosphorylate β-catenin at specific serine and threonine residues. Phosphorylated β-catenin is ubiquitinated and subsequently degraded by the 26S proteasome. Wnt ligands stimulate cells by binding to the cell surface receptor Frizzled and its co-receptors low-density lipoprotein (LDL) receptor-related protein 5/6 (LRP5/6) [7, 8]. Subsequently, the signal mediator Dishevelled (Dsh) is activated leading to a partial inhibition [9, 10] of β-catenin phosphorylation in the destruction complex by a yet unresolved mechanism [6, 11, 12]. As a result, β-catenin accumulates in the cytosol and translocates into the nucleus. There it interacts with transcription factors of the T-cell factor/lymphoid enhancer factor (TCF) family to regulate target gene expression [3, 13]. Aberrant activation of Wnt/ β-catenin signalling is found in several human diseases such as neurodegenerative diseases, type II diabetes, and colon cancer and is often associated with mutations in pathway components [14, 15]. For instance, truncation mutations of APC are frequently detected in colon cancer samples [15, 16]. Wnt/ β-catenin signalling has been subject to several mathematical modelling approaches exploiting the interrelation between transcriptional and adhesive functions of β-catenin, the consequences of carcinogenic mutations of pathway components or subcellular compartmentalisation [17-21].

Ubiquitination of β-catenin is mediated by β-Transducin repeat-containing proteins (β-TrCP) [5, 22] for which in mammalian cells two paralogues, β-TrCP1 and β-TrCP2, with high sequence similarity exist [23, 24] (alternatively referred to as FWD1 and Homologous to Slimb (HOS), respectively [4, 25, 26]). The β-TrCP paralogues constitute the F-box protein subunit of Skp/Cullin/F-box(SCF)-type E3 ubiquitin ligase complexes that mediates the substrate specificity in the ubiquitination process [27-29]. The observed lethality upon simultaneous deletion of both FWD1 and HOS in mice [21, 30] underscores their importance for proper control of β-catenin degradation and, consequently, Wnt/ β-catenin signalling. Generally, FWD1 and HOS are considered to be functionally redundant in regulating β-catenin stability [24-26, 31]. This notion has been inferred from (i) identical biochemical properties of the paralogues [26, 30], (ii) their apparent reciprocal substitution in paralogue-specific small interfering RNA (siRNA)-mediated knock-down experiments [31], and (iii) the viability of FWD1 knock-out mice [26, 31, 32]. Nonetheless, the potential advantage that the presumed functional redundancy could offer is still debated [30].

Compensation by one β-TrCP paralogue for the loss of the other could explain the absence of phenotypic changes upon single knock-out of either the FWD1 or HOS gene in many tissues. However, the testis provides an example where this compensatory mechanism seemingly does not work [31, 33]. Precisely what determines whether or not FWD1 and HOS can substitute for each other is not yet known but context-dependent differences in the

expression and regulation of FWD1 and HOS could play a role. Both β-TrCP paralogues are thought to be expressed at low levels [25] in cell-type specific patterns: HOS is the predominant paralogue found in wild type tissues [25, 34, 35], whereas FWD1 is predominantly detected in primary tumours and cancer cell lines. In addition, HOS and FWD1 expression is controlled by the Wnt/β-catenin signalling pathway itself [34, 36-38], albeit in opposite ways. The expression and activity of HOS is directly inhibited by Wnt/β-catenin signalling [34]. In contrast, FWD1 is up-regulated in response to Wnt/β-catenin signalling via an indirect mechanism: its mRNA is protected from degradation by the coding region determinant-binding protein (CRD-BP), which by itself is a direct target gene product of Wnt/β-catenin signalling [36-38]. Thus, the two β-TrCP paralogues may establish interlocked positive and negative feedback loops. Furthermore, besides Wnt/β-catenin signalling, other signalling pathways have been reported to change the expression levels of the two β-TrCP paralogues [36, 39-41]. Although, control of FWD1 and HOS expression levels by Wnt/β-catenin signalling or other signalling pathways is considered to be a very important factor in the regulation of Wnt/β-catenin signalling [25, 30, 36], cellular FWD1 or HOS concentrations have not yet been quantified. Taken together, the phenotypic consequences of FWD1 and HOS single knock-outs and the cellular responses to Wnt stimulation could be influenced by (i) differential expression of the two paralogues in different tissues under wild-type and pathological conditions, (ii) by the interlocked positive and negative feedback loops established by HOS and FWD1, and (iii) by the cross-regulation of FWD1 and HOS expression levels by other signalling pathways. However, the significance of these regulatory mechanisms and their potential impact on Wnt/β-catenin signalling dynamics and FWD1 and HOS knock-out phenotypes has not yet been investigated.

Here, we have taken a mathematical modelling approach to address the issues. We extend a detailed kinetic model [9] by the two transcriptional feedback mechanisms acting via HOS as well as via CRD-BP and FWD1 to explore the potential impact of differential expression levels and feedback strengths on the dynamics of Wnt/β-catenin signalling. This approach allowed to dissect the specific effects of each individual feedback and demonstrates that predominantly the HOS feedback affects Wnt/β-catenin signalling dynamics in wild type cells while the FWD1 feedback can establish a compensation mechanism to prevent strong β-catenin up-regulation in case of reduced HOS concentration. The presented model thus provides a unifying theoretical framework that allows integrating all the available experimental results and the proposed molecular mechanisms from separate investigations. The model furthermore shows that the FWD1 feedback provides no protection against aberrant Wnt/β-catenin pathway activation in APC mutant cancer cells indicating that pharmaceutical up-regulation of β-TrCP paralogues is unlikely to represent an effective treatment strategy.

3. Results

3.1 Development of a Wnt/β-catenin pathway model that includes the FWD1 and HOS feedback mechanisms

To investigate the regulatory impact of the two transcriptional feedback mechanisms acting via HOS and FWD1, a detailed model of the Wnt/β-catenin signalling pathway [9], which describes the temporal behaviour of the concentrations of central pathway components using ordinary differential equations (ODEs), is modified and extended. A schematic representation of the resulting feedback model is shown in Figure 1. In the scheme, the reactions marked in black are those adopted from the published model of Wnt/β-catenin signalling; the reactions marked in green and blue indicate the newly introduced HOS and FWD1 feedback mechanisms, respectively. The HOS and FWD1 feedback mechanisms are implemented such that FWD1 is indirectly up-regulated by Wnt/β-catenin signalling via the induction of CRD-BP, whereas the transcription of HOS is directly inhibited by the β-catenin/TCF complex. The HOS and FWD1 mediated process of β-catenin ubiquitination is explicitly incorporated into the destruction core cycle of the extended model (Figure 1, reactions 10, 10b, 22, and 22b). The originally published model limits the possible β-catenin/TCF complex concentration by a conservation relation of TCF. To lift this restriction, production and degradation processes of TCF are introduced (reactions 31 and 32, respectively). The resulting model consists of 20 ODEs and three conservation relations (Equations [1] – [23], supplementary Doc. S1, Section 2). A detailed description, motivation and discussion of the model structure are provided in Section 1.1 in the supplementary Doc. S1.

The transcription of HOS mRNA (reaction 18 in Figure 1) and degradation of FWD1 mRNA (reaction 27) are modelled by rate equations that include inhibitory terms (Equations [42] and [53], supplementary Doc. S1, Section 2). The corresponding inhibition constants k_i and k_{i2} modulate the repressive impact of the β-catenin/TCF complex on HOS mRNA production and of CRD-BP on FWD1 mRNA degradation, respectively. Therefore, the inverse of k_i is defined as the HOS feedback strength; likewise, the inverse of k_{i2} is defined as FWD1 feedback strength. For each feedback, it holds that an increasing inhibition constant lowers the repressive impact and thus reduces the feedback strength.

To parameterise the model, several parameters are directly adopted from the originally published model of the Wnt/β-catenin signalling pathway [9] (Tables S2-S3, supplementary Doc. S1). Most remaining parameters are either set to values published in the literature or

estimated from published experimental data (further details in supplementary Doc. S1, Section 1.3). For a few parameters of the reactions involved in the HOS and FWD1 feedback mechanisms no estimates could be deduced from literature. They are set in such a way that the following three experimental observations are obeyed. First, both β-TrCP paralogues have identical biochemical properties in controlling β-catenin stability [26, 31, 32]. Second, both β-TrCP paralogues are expressed at low levels [25]. Third, parameters were chosen such that the reported relative expression patterns of both β-TrCP paralogues in wild type and tumour tissues [25, 34, 35] are reproduced in model simulations. To validate this specification, steady state concentrations of FWD1 and HOS are calculated under wild type and APC mutant conditions. To model APC mutations, parameter sets for 13 different APC mutants (referred to as "m1" to "m13") have been proposed [18]. They are considered to represent different realisations of APC truncation mutations that were detected in colon cancer samples [42, 43]. To simulate one representative mutant condition in the feedback model, the parameter set of APC mutant "m7" (Table S4, supplementary Doc. S1) is chosen. The comparison of the calculated steady state concentrations of FWD1 and HOS (Figure 2A) confirms a lower expression of FWD1 compared to HOS under wild type condition ($6.7 \cdot 10^{-3}$ nM and $9.1 \cdot 10^{-2}$ nM, respectively) but lower expression of HOS than FWD1 under APC mutant condition ($3.0 \cdot 10^{-5}$ nM and $1.0 \cdot 10^{-1}$ nM, respectively). In these calculations, a representative HOS and FWD1 feedback strength of 0.6 nM^{-1} is considered. Other feedback strengths ranging from 0.1 nM^{-1} to 6 nM^{-1} were also used in simulations and yielded similar results for the representative APC mutant condition "m7" as well as other APC truncation mutations (Figure 2B). This shows that the feedback model qualitatively reproduces the differential expression patterns of HOS and FWD1. Whether these predicted concentrations of HOS or FWD1 also meet measured values of cellular concentrations needs to be validated in future experiments. The reference parameter set as well as a detailed explanation of the model parameterisation considering wild type and APC mutant conditions are provided in Section 1.3 of supplementary Doc. S1.

In order to investigate signal transduction dynamics of the Wnt/β-catenin signalling pathway, a transient Wnt stimulus is assumed in the model (Equation [61], supplementary Doc. S1), since it has been argued that pathway activation *in vivo* is transient, likely due to receptor inactivation or other signal down-regulating processes [9, 44-46]. In the model, a transient Wnt stimulus implicates that the steady state upon stimulation is equal to the initial unstimulated steady state (see supplementary Doc. S1, Section 1.4).

3.2 Variation of feedback strength allows for feedback-specific modulation of HOS or FWD1 expression

To dissect the individual impact of each feedback, an influence of the respective other feedback needs to be prevented. This is accomplished by strongly increasing the associated inhibition constant. In the extreme case that an inhibition constant approaches infinity, the limit of the corresponding feedback strength is zero. Consequently, changes in the concentration of the β-catenin/TCF complex (or CRD-BP) have no impact on the concentrations of HOS mRNA (or FWD1 mRNA) under the respective condition. To facilitate numerical calculations in the model analysis, the rate equations of reactions 18 and 27 (Equations [42] and [53], respectively, supplementary Doc. S1) are substituted by Equations [43] and [54], respectively, which is equivalent to setting the respective feedback strength to zero. In Equations [43] and [54], HOS and FWD1 expression is independent of changes in the concentration of the β-catenin/TCF complex and, in consequence, the concentrations of HOS or FWD1 stay at their initial steady state values. That means that the respective feedback regulation is disabled if the corresponding feedback strength is set to zero.

At first, the influence of the individual feedback strengths on the steady state concentration of HOS and FWD1 is analysed under wild type conditions. Therefore, two cases are considered. First, the HOS feedback strength is varied and the FWD1 feedback strength is set to zero (referred to as scenario I); second, the HOS feedback strength is set to zero and the FWD1 feedback strength is varied (referred to as scenario II). The simulations of scenario I show that increasing HOS feedback strength decreases the steady state concentration of HOS (Figure 3A) due to the repressive impact of β-catenin/TCF on the production of HOS mRNA. In scenario II, increasing FWD1 feedback strength increases the steady state concentration of FWD1 (Figure 3B) due to the positive regulation of FWD1 by the β-catenin/TCF complex. In both scenarios (I and II) a variation of feedback strength does not change the steady state concentration of the respective other β-TrCP paralogue.

The analysis demonstrates that variation of the individual feedback strength allows for feedback-specific modulation of either HOS or FWD1 expression if the respective other feedback strength is set to zero. Note that the steady state concentrations of HOS and FWD1 differ considerably (1.6 nM and $5.2 \cdot 10^{-6}$ nM, respectively) if the respective feedback strength is set to zero. In the following sections, the individual impacts of the HOS and FWD1 feedbacks on the β-catenin/TCF complex, as the transcriptionally active readout of the pathway model, are investigated.

3.3 HOS feedback strength affects β-catenin/TCF steady state concentration and its dynamics upon Wnt stimulation

To investigate the impact of the HOS feedback on the steady state concentration of the β-catenin/TCF complex, scenario I is examined again. The simulations show that HOS feedback strengths of less than 1 nM^{-1} maintain a low steady state concentration of the β-catenin/TCF complex of about 6.9 nM, whereas HOS feedback strengths greater than 1 nM^{-1} result in an accumulation of β-catenin/TCF complexes (Figure 4A). As shown in Figure 3A, increasing HOS feedback strengths reduce the HOS protein concentration. Consequently, the HOS-dependent β-catenin degradation is strongly inhibited resulting in the accumulation of β-catenin/TCF complexes up to a concentration of about 390 nM. In the intermediate range of HOS feedback strength (about 1 - 10 nM^{-1}), multiple β-catenin/TCF steady state solutions are possible (Materials and Methods). An analysis of the stability of the steady state solutions reveals that only the highest β-catenin/TCF concentration belongs to the stable solution observable in experiments (Materials and Methods). Thus, the steady state concentration of the β-catenin/TCF complex changes in a switch-like manner to alterations in HOS feedback strength. This implies in particular, that the steady state concentration of the β-catenin/TCF complex is strongly increased even in the absence of any Wnt stimulus if the HOS feedback strength exceeds a critical value.

The HOS feedback strength also affects the dynamics of the β-catenin/TCF complex upon transient Wnt stimulation (Figure 4B). To quantify the impact of the HOS feedback strength on the dynamics, three measures are considered (see Materials and Methods Section 4.2) that characterise typical properties of transient signal-response dynamics: signalling time, signal duration as well as signal amplitude [47]. The signalling time may be interpreted as the expected time that the signal of the Wnt stimulus needs to arrive at the level of the β-catenin/TCF complex in the pathway [48]. Signal duration refers to the duration of the β-catenin/TCF complex concentration change upon transient Wnt stimulation and signal amplitude to the magnitude of the concentration change [48]. These three measures are calculated for the dynamics of the β-catenin/TCF complex upon transient Wnt stimulation considering HOS feedback strengths ranging from 10^{-2} nM^{-1} to 1 nM^{-1} (Figure 4C). The values of signalling time, signal duration, and signal amplitude for the HOS feedback strength of 10^{-2} nM^{-1} are very similar to those values calculated if both feedback strengths are set to zero (430 min, 434 min, and 2.9 nM, respectively). If the HOS feedback strength is increased to 1 nM^{-1}, the signalling time increases about 2.4-fold, β-catenin/TCF signal duration extends about 1.8-fold, and β-catenin/TCF signal amplitude enhances by about 40% (Figure 4C). Addressing HOS feedback strengths above 1 nM^{-1}, the high steady state

concentration of the β-catenin/TCF complex (Figure 4A) is maintained over time upon transient Wnt stimulation (shown for a representative HOS feedback strength of 60 nM^{-1} in Figure 6A). This indicates that HOS feedback strengths above 1 nM^{-1} render the β-catenin/TCF complex non-responsive to Wnt stimulation.

Taken together, enhancing HOS feedback strengths up to 1 nM^{-1} leads to a low steady state concentration of the β-catenin/TCF complex but increases signalling time, signal duration as well as signal amplitude of the β-catenin/TCF complex dynamics upon transient Wnt stimulation. If the HOS feedback strength exceeds 1 nM^{-1}, the steady state concentration of the β-catenin/TCF complex is high independent of a Wnt stimulus and does not change upon transient Wnt stimulation.

3.4 FWD1 feedback strength does not affect the dynamics of the β-catenin/TCF complex for the presumed HOS expression level

To determine the regulatory influence of the FWD1 feedback on the β-catenin/TCF dynamics, scenario II is revisited. Although variation of the FWD1 feedback strength changes FWD1 concentration (Figure 3B), no influence of the FWD1 feedback strength on the steady state concentration of the β-catenin/TCF complex is observed (Figure 5A). Furthermore, β-catenin/TCF dynamics in response to transient Wnt stimulation appear unaffected by changes of FWD1 feedback strength in the range from 10^{-2} nM^{-1} to 1 nM^{-1} (Figure 5B). Signalling time, signal duration, and signal amplitude of the β-catenin/TCF complex dynamics stay almost constant at 430 min, 434 min, and 2.9 nM, respectively (Figure 5C). This insensitivity of the β-catenin/TCF complex dynamics towards changes in the FWD1 feedback strength is due to the constant HOS concentration of about 1.6 nM. This HOS concentration compensates for the low FWD1 concentrations (less than $1.1 \cdot 10^{-2}$ nM) in the case of FWD1 feedback strengths of less than 1 nM^{-1} (Figure 3B). In the case of FWD1 feedback strengths above 10 nM^{-1}, increased FWD1 concentrations (higher than 0.1 nM) in addition to the HOS concentration of about 1.6 nM do also not affect β-catenin/TCF dynamics (Figure 5C).

The analysis shows that the HOS concentration in scenario II is too high to observe effects of changes in FWD1 feedback strength. Since increasing HOS feedback strength reduces HOS concentrations (Figure 3A), different combinations of HOS and FWD1 feedback strength are addressed in the next section to examine a potential influence of FWD1 feedback strength under conditions of reduced HOS expression.

3.5 The FWD1 feedback influences steady state concentration and dynamics of the β-catenin/TCF complex in the case of reduced HOS expression

To investigate whether an impact of the FWD1 feedback strength becomes observable under the condition of reduced HOS expression, the HOS feedback strength is set to 60 nM^{-1}. As demonstrated before, combining this HOS feedback strength with a FWD1 feedback strength of zero results in a strong increase of the steady state concentration of the β-catenin/TCF complex (Figure 4A and Figure 6B), which is maintained over time upon transient Wnt stimulation (Figure 6A). If, however, this HOS feedback strength of 60 nM^{-1} is combined with a FWD1 feedback strength of 60 nM^{-1}, the steady state concentration of the β-catenin/TCF complex decreases to 6.9 nM (Figure 6B), which is equal to the steady state concentration of the β-catenin/TCF complex corresponding to HOS feedback strengths of less than 1 nM^{-1} (Figure 4A). Moreover, setting both feedback strengths to 60 nM^{-1} restores the transient increase of the β-catenin/TCF complex concentration upon transient Wnt stimulation (Figure 6C), which is otherwise not observable for HOS feedback strengths of 60 nM^{-1} if the FWD1 feedback strength is set to zero (Figure 6A).

Additional simulations that consider different combinations of HOS and FWD1 feedback strengths below 1 nM^{-1} also demonstrate that increasing FWD1 feedback strengths can reduce the impact of the HOS feedback strength on the dynamics of the β-catenin/TCF complex (Fig. S1). Increasing HOS feedback strength up to 1 nM^{-1} approximately doubles the signalling times from 430 min to 890 min, increases the signal durations from 434 min to 696 min, and enhances the signal amplitudes from 2.9 nM to 4.0 nM (Fig. S1D-F, respectively). These influences of the HOS feedback strength are partially counteracted by FWD1 feedback strengths up to 1 nM^{-1}, reducing signalling time, signal duration, and signal amplitude to intermediate values (Fig. S1D-F, respectively).

The analysis shows that the effects of the HOS feedback strength on the β-catenin/TCF complex can be counteracted by enhanced FWD1 feedback strength demonstrating that the impact of FWD1 feedback strength becomes observable under the condition of reduced HOS expression.

3.6 Up-regulation of FWD1 or HOS expression level reduces the effects of the HOS feedback on β-catenin/TCF complex dynamics

In the previous sections, the expression level of FWD1 was increased by enhancing FWD1 feedback strength (Figure 3B), which describes its regulation dependent on Wnt/β-catenin

signalling. However, experiments indicate that the expression level of FWD1 may also be enhanced by stress-induced c-Jun N-terminal kinase (JNK) signalling or Akt/Protein Kinase B (PKB) signalling. In the feedback model, FWD1 concentration can be increased in a β-catenin/TCF-independent manner by increasing the FWD1 mRNA production rate v_{28}. The simulations show that a higher FWD1 mRNA production rate decreases signalling time, signal duration, and signal amplitude of the dynamics of the β-catenin/TCF complex upon transient Wnt stimulation (Figure 7A, dark red line) compared to the dynamics corresponding to the reference FWD1 mRNA production rate (red line). For example, a 10-fold increase of the FWD1 mRNA production rate leads to a decrease of the signalling time by about 15%, of the signal duration by about 10%, and of the signal amplitude by about 5% (Figure 7B, dark red lines).

Considering HOS expression, simulations show that a higher HOS mRNA production rate $vmax_{18}$ decreases signalling time, signal duration, and signal amplitude of the β-catenin/TCF dynamics upon transient Wnt stimulation to a larger extent compared to FWD1 (Figure 7A, orange line). Already a small increase of HOS mRNA production rate by only 2-fold results in about 14% decrease of the signalling time, about 8% decrease of signal duration, and about 6% decrease of the signal amplitude (Figure 7B, orange lines). In the extreme case of transcriptional up-regulation of FWD1 and/or HOS of greater than 10-fold, signalling time, signal duration, and signal amplitude of the β-catenin/TCF complex dynamics decrease to the values of the dynamics with HOS and FWD1 feedback strengths set to zero (430 min, 434 min, and 2.9 nM, respectively; Fig. S2). This indicates that transcriptional up-regulation of FWD1 or HOS in a β-catenin/TCF-independent manner reduces the impact of the HOS feedback on the dynamics of the β-catenin/TCF complex upon transient Wnt stimulation.

3.7 The FWD1 feedback mechanism does not protect against up-regulation of β-catenin/TCF complex concentrations induced by APC mutations

So far, the impact of the FWD1 and HOS feedback has been discussed in the case of wild type cells that are characterised by a much lower concentration of FWD1 than of HOS. The analyses have shown that under wild type conditions the potential impact of the FWD1 feedback on the steady state concentration and dynamics of the β-catenin/TCF complex is masked by the present HOS concentration. In contrast to wild type cells, primary tumours and cancer cell lines hardly express HOS [25, 35]. Thus, FWD1 feedback effects might become observable under that condition. To simulate cancerous conditions, published parameter sets of APC truncation mutants [18] were adopted within the feedback

model (supplementary Doc. S1, Section 1.3). The simulations show that the steady state concentrations of the β-catenin/TCF complex are increased in all APC mutants compared to wild type condition if the FWD1 feedback strength is set to zero in combination with a HOS feedback strength between 0.1 nM^{-1} and 1 nM^{-1} (Figure 8A). To explore whether the FWD1 feedback might provide a protection mechanism against aberrant activation of Wnt/β-catenin signalling in cells harbouring an APC mutation, the FWD1 feedback is set to feedback strengths in the range of 0.1 nM^{-1} to 6 nM^{-1}. The simulations show that the steady state concentration of FWD1 for each APC mutant condition is increased compared to its steady state concentration under wild type conditions, despite the absence of a Wnt stimulus (Figure 8C). Dependent on the particular APC mutant, the fold increase of FWD1 spans from merely 1.1-fold for APC mutant "m1" to approximately 17-fold for APC mutants "m9" to "m13" (Figure 8D). Calculating the corresponding steady state concentration of the β-catenin/TCF complex for the wild type and each APC mutant shows that the steady state concentrations of the β-catenin/TCF complex hardly change if the FWD1 feedback strength is set in the range of 0.1 nM^{-1} to 6 nM^{-1} (Figure 8B) compared to those concentrations calculated for the FWD1 feedback strength set to zero (Figure 8A). This is also observed for other combinations of parameter values than the particular values published for APC truncation mutants "m1" to "m13" (Fig. S3). Taken together, the results indicate that the FWD1 feedback mechanism probably does not protect against up-regulated steady state concentration of the β-catenin/TCF complex due to mutations of APC.

4. Discussion

Transcriptional regulation of the expression of the β-TrCP paralogues HOS and FWD1 by Wnt/β-catenin signalling realises two transcriptional feedback mechanisms in the Wnt/β-catenin pathway. In this study, the regulatory impact of the HOS and FWD1 feedbacks on the dynamics of Wnt/β-catenin signalling was investigated. The modelling approach allowed the discrimination between the particular influences of each individual feedback by modulating its respective feedback strength. The analysis demonstrated that the opposite regulation of HOS and FWD1 expression levels by the β-catenin/TCF complex results in distinct regulatory influence of the two feedbacks on the dynamics of the β-catenin/TCF complex. It furthermore showed that the actual impact of each feedback strongly depends on the expression levels of HOS and FWD1.

The presented feedback model is derived from a model that quantitatively reproduced experimental data [9]. Since currently available information on HOS and FWD1 considered in our modelling approach is qualitative, the presented results should also be understood as qualitative. Most model parameters were set to values collected in an extensive literature

search. They originate from mammalian cell types as well as from extracts of *Xenopus* oocytes, since no comprehensive experimental time series data sets are available to estimate the kinetic parameters of a specific mammalian cell type. Recent experiments on the quantification of pathway components in resting mammalian cells show that key components such as Axin, APC, and β-catenin may be expressed in a highly cell-type specific manner [49-53], which may have consequences on signalling dynamics and downstream gene expression. From this point of view, a comprehensive quantitative analysis of the Wnt/β-catenin pathway would be desirable. Irrespective of this, the feedback model presented here accurately reproduces experimental data (Figure 2A). Comprehensive variations of multiple model parameters in the simulations lead to similar results demonstrating that the model predictions are largely independent from the particular choice of the model parameter set.

In wild type cells, higher concentrations of HOS than of FWD1 have been detected [25, 34, 35]. On the basis of this experimental finding, the model predicts that under wild type conditions primarily the HOS feedback influences the dynamics of the β-catenin/TCF complex in response to transient Wnt stimulation. Increasing HOS feedback strengths up to 1 nM^{-1} increased the signalling time, signal duration, and amplitude of the dynamics of the β-catenin/TCF complex upon transient Wnt stimulation (Figure 4B and C), which indicates a change in the response of the Wnt/β-catenin pathway to Wnt stimulation. Increasing HOS feedback strengths above 1 nM^{-1} increased the steady state concentration of the β-catenin/TCF complex in a switch-like manner (Figure 4A). In that case, a Wnt stimulus does not induce an observable concentration change of the β-catenin/TCF complex (Figure 6A). This indicates that HOS feedback strengths above 1 nM^{-1} render the β-catenin/TCF complex concentration non-responsive to Wnt stimulation. To experimentally validate the predictions one could try to vary HOS feedback strength by modulating the transcriptional efficiency of the β-catenin/TCF complexes. This could be achieved by applying decoy oligonucleotides [54]. Decoy oligonucleotides are short synthetic double-stranded DNA molecules that can competitively inhibit the interaction of TCF with promoters and thus modulate target gene expression. In the case of HOS mRNA, decoy oligonucleotides could therefore reduce the inhibitory impact of β-catenin/TCF complexes on HOS mRNA expression. The model analysis predicts that titration of decoy oligonucleotides affects the dynamics of the β-catenin/TCF complex upon transient Wnt stimulation (Figure 4B and C). This may be best observed in CRD-BP knock-out cells since in these cells regulation of FWD1 by β-catenin/TCF is abolished. Thus, CRD-BP knock-out cells represent the scenario of FWD1 feedback strength set to zero. In CRD-BP knock-out cells, the titration of decoy oligonucleotides in combination with siRNA-mediated HOS knock-down (FA) may also be

used to experimentally validate the switch-like response of the β-catenin/TCF steady state concentration predicted by the model (Figure 4A).

The model furthermore predicted that the FWD1 feedback by itself cannot influence the β-catenin/TCF dynamics in wild type cells due to the reported HOS expression levels that by themselves already ensure adequate β-catenin degradation independent of the present FWD1 concentration (Figure 5). This result is in line with the reported experimental observation that already about 10-20% of the cellular HOS concentration can compensate even extreme variations in FWD1 concentration [33]. The model analysis showed that the FWD1 feedback gained regulatory impact on steady state concentration and dynamics of the β-catenin/TCF complex under the condition of further reduced HOS concentration (Figure 6). HOS feedback strengths above 1 nM^{-1} strongly reduce the steady state concentrations of HOS (Figure 3A). Such a reduced HOS concentration interferes with the degradation of β-catenin via the HOS-dependent mechanism resulting in the strong increase of β-catenin/TCF concentrations if the FWD1 feedback strength is set to zero (Figure 4A and Figure 6B). If, however, the FWD1 feedback strength is increased to a value above zero, enhanced β-catenin/TCF complex concentrations up-regulate the FWD1 concentration. This allows for enhanced β-catenin degradation via the β-catenin*/APC*/Axin*/GSK3/FWD1 complex. Consequently, the concentration of the β-catenin/TCF complex is reduced. Moreover, the pathway becomes responsive to Wnt stimulation again (Figure 6). In the same way, the FWD1 feedback may constitute a compensation mechanism against strong up-regulation of β-catenin/TCF complex concentrations due to sequestration of HOS by other substrates such as proteins of the IκB family. The different functions of the FWD1 and HOS feedback mechanisms can be experimentally tested by comparing the effects of single knock-out of FWD1 or HOS in wild type, CRD-BP knock-out (FWD1 feedback strength set to zero), and APC mutant cells (FB). Effects of HOS knock-out are compensated in wild type cells (FB, third bar) through the FWD1 feedback mechanism. If, however, this feedback mechanism is lost, as in CRD-BP knock-out cells, the absence of HOS results in a strong increase of β-catenin/TCF concentrations (sixth bar). In contrast, knock-out of FWD1 hardly affects β-catenin/TCF concentrations in both wild type and CRD-BP knock-out cells since their HOS levels are sufficient to regulate β-catenin concentrations (second and third bar).

Experiments have shown that a knock-down of HOS as well as a knock-out of FWD1 results in almost no observable differences in the murine phenotypes [31]. In terms of the model this means that the steady state and the dynamics of the β-catenin/TCF complex are almost unchanged compared to the wild type condition. The modelling approach demonstrates that two different underlying reasons account for the experimental observations. On the one hand, the down-regulation of the HOS concentration by siRNA treatment is counteracted by the concurrent up-regulation of FWD1 induced by β-catenin/TCF. On the other hand, in the

case of the FWD1 knock-down, its loss is masked by the high concentration of HOS. Hence, under both conditions an adequate amount of total β-TrCP (HOS and FWD1) is available to mediate the degradation of β-catenin and to prevent effects on the phenotype. Experiments with FWD1 knock-out mice have demonstrated that the expression levels of HOS differ in different tissues. In the testis it is low compared to other tissues and the testis is the only tissue that shows phenotypic changes in FWD1 knock-out mice [31, 33]. The modelling approach indicates that if the concentration of HOS is below a critical value, it is not able to compensate for the loss of FWD1 resulting in a higher level of β-catenin/TCF and consequently a phenotypic change. Hence, the model supports the idea that the appearance or non-appearance of a phenotypic effect in FWD1 knock-out mice is caused by the different expression levels of HOS [31, 33].

HOS and FWD1 establish interlocked positive and negative feedback loops in Wnt/β-catenin signalling. Interlocked feedback loops are common network topologies in many biological processes. They are for instance found in the galactose utilization network of *S. cerevisiae* [55], enable stochastic fate decisions in sporulation of *B. subtilis* [56], underlay target gene regulation by Wnt signalling in *C. elegans* [57], are present in p53 signalling [58] and cell cycle regulation networks [59]. Extensive theoretical analyses on dynamical properties of such interlocked feedbacks have been undertaken [60-63]. These studies revealed a diverse set of complex dynamics, covering bistability, excitability, as well as limit-cycle oscillations, and design principles to regulate noise depending on the considered biological processes. The HOS and FWD1 interlocked feedback loops reveal the additional property of a protection mechanism against aberrant pathway activation caused by reduced HOS or FWD1 activity as explained above.

Several human diseases are associated with aberrant activation of Wnt/β-catenin signalling. Despite extensive research, drugs that inhibit aberrant pathway activation are not yet available for clinical use. This is partially due to the lack of accessible enzyme targets in the pathway and the complexity of pathway regulation [14, 64]. In principle, the β-TrCP paralogues could represent useful pharmacological tools to reduce aberrant pathway activation due to their capability to directly target β-catenin and promote its degradation. Indeed, overexpression of FWD1 was shown to promote the down-regulation of β-catenin in cancer cell lines [65]. The model analyses also support that notion by demonstrating that (i) the modulation of HOS and FWD1 expression has a strong regulatory impact on the dynamics of Wnt/β-catenin signalling (Figure 7), and (ii) increased FWD1 concentrations reduced the high β-catenin/TCF concentration that resulted from strong HOS feedbacks under wild type conditions (Figure 6B).

A clinically relevant disease that is associated with aberrant activation of Wnt/β-catenin signalling is colon cancer. Colon cancer cells often harbour mutations in APC that reduce the

efficiency of β-catenin phosphorylation in the destruction complex. Simulations of APC mutations using the feedback model of Wnt/β-catenin signalling showed that the mutation-induced increase of the steady state concentration of β-catenin/TCF is paralleled by a strong up-regulation of the expression level of FWD1 due to the transcriptional control of FWD1 by the β-catenin/TCF complex (Figure 8). This theoretical finding agrees well with experimental observations of increased FWD1 concentration in this cancer type [35, 36, 66]. The simulations furthermore demonstrated that even strongly up-regulated FWD1 concentrations by up to 17-fold increase could not reduce the elevated β-catenin/TCF steady state concentrations under APC mutant conditions (Figure 8). The mutations of APC invincibly interfere with the phosphorylation of β-catenin, which is the prerequisite for the β-TrCP paralogues to mediate β-catenin degradation. Thus, it is reasonable to assume that pharmaceutical up-regulation of either β-TrCP paralogue hardly affects the aberrant activation of the Wnt/β-catenin pathway in APC mutation associated cancer. Moreover, the β-TrCP paralogues regulate several signalling proteins outside of Wnt/β-catenin signalling, such as IκB and Mouse double minute 2 homolog (Mdm2) [24, 25]. Consequently, up-regulation of HOS and/or FWD1 may induce inappropriate signalling responses in the NF-κB and p53 signalling pathways indicating that such an approach generally may not be feasible.

Besides Wnt/β-catenin signalling, also other signalling pathways were reported to contribute to the regulation of HOS and FWD1 expression levels, for instance stress-induced JNK signalling, Akt/PKB signalling, and mitogen-activated protein kinase (MAPK) signalling [36, 39-41]. The model analysis showed that the regulation of HOS or FWD1 concentration by β-catenin/TCF-independent transcriptional activation modulated the β-catenin/TCF complex dynamics (Figure 7, Fig. S2). One may thus speculate that other signalling pathways can influence the duration of β-catenin/TCF complex dynamics via transcriptional regulation of HOS or FWD1 and, in this way, may co-regulate Wnt/β-catenin target gene expression.

4.1 Calculation of steady states and their stability

Numerical calculation of steady states and their stability as well as simulations of dynamics of species were performed using Mathematica 9.0 (Wolfram Research). Steady states are calculated by setting the time derivative of each species concentration in the model to zero and solving the resulting algebraic equation system for the species concentrations. The number of steady states is calculated by counting the steady state solutions that yield non-negative real values of all species concentrations (Fig. S4). To determine the stability of a steady state, the eigenvalues of the Jacobian matrix are calculated [67]. If the real parts of all eigenvalues are negative the steady state is asymptotically stable. Otherwise, the steady state is called unstable.

4.2 Definition of signalling time, signal duration, and signal amplitude

The calculated steady states are used as initial conditions to simulate the continuous dynamics of the model species over time. To quantitatively characterise the dynamics of species in ODE models, several measures have been introduced (reviewed in [47]). Here, three particular measures are considered: signalling time, signal duration, and signal amplitude. These three measures may be interpreted to provide information on (i) the expected time that the signal needs to arrive at the level of pathway readout (signalling time), (ii) the duration of the response at the level of pathway readout (signal duration), and (iii) the magnitude of this response (signal amplitude) [48]. The following definitions of signalling time (Equation [1]), signal duration (Equation [2]), and signal amplitude (Equation [3]) are used that are based on earlier definitions [48, 68, 69]:

$$\text{signalling time} = \frac{\int_{t_{initial}}^{t_{final}} t \cdot \left| \frac{dC[t]}{dt} \right| dt}{\int_{t_{initial}}^{t_{final}} \left| \frac{dC[t]}{dt} \right| dt} \qquad [1]$$

$$\text{signal duration} = \sqrt{\frac{\int_{t_{initial}}^{t_{final}} t^2 \cdot \left|\frac{dC[t]}{dt}\right| dt}{\int_{t_{initial}}^{t_{final}} \left|\frac{dC[t]}{dt}\right| dt} - \left(\frac{\int_{t_{initial}}^{t_{final}} t \cdot \left|\frac{dC[t]}{dt}\right| dt}{\int_{t_{initial}}^{t_{final}} \left|\frac{dC[t]}{dt}\right| dt}\right)^2} \quad [2]$$

$$\text{signal amplitude} = \max C[t] - \min C[t] \qquad t_{initial} \le t \le t_{final} \quad [3]$$

5. Acknowledgements

Studies in this project were funded by the ForSys and Virtual Liver programmes of the German Ministry of Education and Research (grant numbers 0315289 and 0315766), the MSBN project within the Helmholtz Alliance on Systems Biology funded by the Initiative and Networking Fund of the Helmholtz Association. We also thank the graduate school Computational Systems Biology (CSB) of the German Research Foundation (DFG-Graduiertenkolleg 1772).

6. References

1. Inestrosa NC & Arenas E (2010) Emerging roles of Wnts in the adult nervous system. *Nat Rev Neurosci* **11**, 77-86.
2. Clevers H & Nusse R (2012) Wnt/beta-Catenin Signaling and Disease. *Cell* **149**, 1192-1205, doi: http://dx.doi.org/10.1016/j.cell.2012.05.012.
3. Archbold HC, Yang YX, Chen L & Cadigan KM (2012) How do they do Wnt they do?: regulation of transcription by the Wnt/beta-catenin pathway. *Acta Physiol (Oxf)* **204**, 74-109, doi: 10.1111/j.1748-1716.2011.02293.x.
4. Valenta T, Hausmann G & Basler K (2012) The many faces and functions of beta-catenin. *EMBO J* **31**, 2714-2736, doi: emboj2012150 [pii] 10.1038/emboj.2012.150.
5. Saito-Diaz K, Chen TW, Wang X, Thorne CA, Wallace HA, Page-McCaw A & Lee E (2013) The way Wnt works: components and mechanism. *Growth Factors* **31**, 1-31, doi: 10.3109/08977194.2012.752737.
6. Stamos JL & Weis WI (2013) The beta-Catenin Destruction Complex. *Cold Spring Harb Perspect Biol* **5**, doi: 10.1101/cshperspect.a007898.
7. MacDonald BT & He X (2012) Frizzled and LRP5/6 Receptors for Wnt/beta-Catenin Signaling. *Cold Spring Harb Perspect Biol* **4**, doi: 10.1101/cshperspect.a007880.
8. Niehrs C (2012) The complex world of WNT receptor signalling. *Nat Rev Mol Cell Biol* **13**, 767-779.

9. Lee E, Salic A, Kruger R, Heinrich R & Kirschner MW (2003) The roles of APC and Axin derived from experimental and theoretical analysis of the Wnt pathway. *PLoS Biol* **1**, E10, doi: 10.1371/journal.pbio.0000010.
10. Hernandez AR, Klein AM & Kirschner MW (2012) Kinetic responses of beta-catenin specify the sites of Wnt control. *Science* **338**, 1337-1340, doi: 10.1126/science.1228734 science.1228734 [pii].
11. Metcalfe C & Bienz M (2011) Inhibition of GSK3 by Wnt signalling--two contrasting models. *J Cell Sci* **124**, 3537-3544, doi: 10.1242/jcs.091991 124/21/3537 [pii].
12. Tacchelly-Benites O, Wang Z, Yang E, Lee E & Ahmed Y (2013) Toggling a conformational switch in Wnt/beta-catenin signaling: regulation of Axin phosphorylation. The phosphorylation state of Axin controls its scaffold function in two Wnt pathway protein complexes. *Bioessays* **35**, 1063-1070, doi: 10.1002/bies.201300101.
13. Hecht A & Kemler R (2000) Curbing the nuclear activities of beta-catenin. Control over Wnt target gene expression. *EMBO Rep* **1**, 24-28, doi: 10.1093/embo-reports/kvd012.
14. Zimmerman ZF, Moon RT & Chien AJ (2012) Targeting Wnt pathways in disease. *Cold Spring Harb Perspect Biol* **4**, doi: 10.1101/cshperspect.a008086.
15. Giles RH, van Es JH & Clevers H (2003) Caught up in a Wnt storm: Wnt signaling in cancer. *Biochim Biophys Acta* **1653**, 1-24, doi: S0304419X03000052 [pii].
16. Polakis P (2012) Wnt signaling in cancer. *Cold Spring Harb Perspect Biol* **4**, doi: 10.1101/cshperspect.a008052 a008052 [pii] cshperspect.a008052 [pii].
17. van Leeuwen IMM, Byrne HM, Jensen OE & King JR (2007) Elucidating the interactions between the adhesive and transcriptional functions of [beta]-catenin in normal and cancerous cells. *J Theor Biol* **247**, 77-102.
18. Cho KH, Baek S & Sung MH (2006) Wnt pathway mutations selected by optimal beta-catenin signaling for tumorigenesis. *FEBS Lett* **580**, 3665-3670, doi: S0014-5793(06)00666-1 [pii] 10.1016/j.febslet.2006.05.053.
19. Benary U, Kofahl B, Hecht A & Wolf J (2013) Modelling Wnt/ß-catenin target gene expression in APC and Wnt gradients under wild type and mutant conditions. *Frontiers in Physiology* **4**, doi: 10.3389/fphys.2013.00021.
20. Schmitz Y, Rateitschak K & Wolkenhauer O (2013) Analysing the impact of nucleo-cytoplasmic shuttling of β-catenin and its antagonists APC, Axin and GSK3 on Wnt/β-catenin signalling. *Cellular Signalling*, doi: http://dx.doi.org/10.1016/j.cellsig.2013.07.005.
21. Barua D & Hlavacek WS (2013) Modeling the effect of APC truncation on destruction complex function in colorectal cancer cells. *PLoS Comput Biol* **9**, e1003217, doi: 10.1371/journal.pcbi.1003217 PCOMPBIOL-D-13-00274 [pii].
22. Tauriello DV & Maurice MM (2010) The various roles of ubiquitin in Wnt pathway regulation. *Cell Cycle* **9**, 3700-3709, doi: 13204 [pii] 10.4161/cc.9.18.13204.
23. Seo E, Kim H, Kim R, Yun S, Kim M, Han JK, Costantini F & Jho EH (2009) Multiple isoforms of beta-TrCP display differential activities in the regulation of Wnt signaling. *Cell Signal* **21**, 43-51, doi: S0898-6568(08)00269-6 [pii] 10.1016/j.cellsig.2008.09.009.
24. Lau AW, Fukushima H & Wei W (2012) The Fbw7 and betaTRCP E3 ubiquitin ligases and their roles in tumorigenesis. *Frontiers in bioscience : a journal and virtual library* **17**, 2197-2212.

25. Fuchs SY, Spiegelman VS & Kumar KG (2004) The many faces of beta-TrCP E3 ubiquitin ligases: reflections in the magic mirror of cancer. *Oncogene* **23**, 2028-2036, doi: 10.1038/sj.onc.1207389
1207389 [pii].
26. Frescas D & Pagano M (2008) Deregulated proteolysis by the F-box proteins SKP2 and beta-TrCP: tipping the scales of cancer. *Nat Rev Cancer* **8**, 438-449, doi: nrc2396 [pii]
10.1038/nrc2396.
27. Maniatis T (1999) A ubiquitin ligase complex essential for the NF-kappaB, Wnt/Wingless, and Hedgehog signaling pathways. *Genes Dev* **13**, 505-510.
28. Ciechanover A, Orian A & Schwartz AL (2000) Ubiquitin-mediated proteolysis: biological regulation via destruction. *Bioessays* **22**, 442-451, doi: 10.1002/(SICI)1521-1878(200005)22:5<442::AID-BIES6>3.0.CO;2-Q.
29. Deshaies RJ & Joazeiro CA (2009) RING domain E3 ubiquitin ligases. *Annu Rev Biochem* **78**, 399-434, doi: 10.1146/annurev.biochem.78.101807.093809.
30. Kanarek N & Ben-Neriah Y (2012) Regulation of NF-kappaB by ubiquitination and degradation of the IkappaBs. *Immunol Rev* **246**, 77-94, doi: 10.1111/j.1600-065X.2012.01098.x.
31. Guardavaccaro D, Kudo Y, Boulaire J, Barchi M, Busino L, Donzelli M, Margottin-Goguet F, Jackson PK, Yamasaki L & Pagano M (2003) Control of meiotic and mitotic progression by the F box protein beta-Trcp1 in vivo. *Dev Cell* **4**, 799-812, doi: S1534580703001540 [pii].
32. Nakayama K, Hatakeyama S, Maruyama S, Kikuchi A, Onoe K, Good RA & Nakayama KI (2003) Impaired degradation of inhibitory subunit of NF-kappa B (I kappa B) and beta-catenin as a result of targeted disruption of the beta-TrCP1 gene. *Proc Natl Acad Sci U S A* **100**, 8752-8757, doi: 10.1073/pnas.1133216100
1133216100 [pii].
33. Kanarek N, Horwitz E, Mayan I, Leshets M, Cojocaru G, Davis M, Tsuberi BZ, Pikarsky E, Pagano M & Ben-Neriah Y (2010) Spermatogenesis rescue in a mouse deficient for the ubiquitin ligase SCF{beta}-TrCP by single substrate depletion. *Genes Dev* **24**, 470-477, doi: 24/5/470 [pii]
10.1101/gad.551610.
34. Spiegelman VS, Tang W, Katoh M, Slaga TJ & Fuchs SY (2002) Inhibition of HOS expression and activities by Wnt pathway. *Oncogene* **21**, 856-860, doi: 10.1038/sj.onc.1205132.
35. Saitoh T & Katoh M (2001) Expression profiles of betaTRCP1 and betaTRCP2, and mutation analysis of betaTRCP2 in gastric cancer. *Int J Oncol* **18**, 959-964.
36. Spiegelman VS, Slaga TJ, Pagano M, Minamoto T, Ronai Z & Fuchs SY (2000) Wnt/beta-catenin signaling induces the expression and activity of betaTrCP ubiquitin ligase receptor. *Mol Cell* **5**, 877-882, doi: S1097-2765(00)80327-5 [pii].
37. Noubissi FK, Elcheva I, Bhatia N, Shakoori A, Ougolkov A, Liu J, Minamoto T, Ross J, Fuchs SY & Spiegelman VS (2006) CRD-BP mediates stabilization of betaTrCP1 and c-myc mRNA in response to beta-catenin signalling. *Nature* **441**, 898-901, doi: nature04839 [pii]
10.1038/nature04839.
38. Elcheva I, Goswami S, Noubissi FK & Spiegelman VS (2009) CRD-BP protects the coding region of betaTrCP1 mRNA from miR-183-mediated degradation. *Mol Cell* **35**, 240-246, doi: S1097-2765(09)00398-0 [pii]
10.1016/j.molcel.2009.06.007.

39. Spiegelman VS, Stavropoulos P, Latres E, Pagano M, Ronai Z, Slaga TJ & Fuchs SY (2001) Induction of beta-transducin repeat-containing protein by JNK signaling and its role in the activation of NF-kappaB. *J Biol Chem* **276**, 27152-27158, doi: 10.1074/jbc.M100031200 M100031200 [pii].
40. Zhang M, Yan Y, Lim YB, Tang D, Xie R, Chen A, Tai P, Harris SE, Xing L, Qin YX, et al. (2009) BMP-2 modulates beta-catenin signaling through stimulation of Lrp5 expression and inhibition of beta-TrCP expression in osteoblasts. *J Cell Biochem* **108**, 896-905, doi: 10.1002/jcb.22319.
41. Spiegelman VS, Tang W, Chan AM, Igarashi M, Aaronson SA, Sassoon DA, Katoh M, Slaga TJ & Fuchs SY (2002) Induction of homologue of Slimb ubiquitin ligase receptor by mitogen signaling. *J Biol Chem* **277**, 36624-36630, doi: 10.1074/jbc.M204524200 M204524200 [pii].
42. Kikuchi A (2003) Tumor formation by genetic mutations in the components of the Wnt signaling pathway. *Cancer Sci* **94**, 225-229.
43. Kohler EM, Brauburger K, Behrens J & Schneikert J (2010) Contribution of the 15 amino acid repeats of truncated APC to [beta]-catenin degradation and selection of APC mutations in colorectal tumours from FAP patients. *Oncogene* **29**, 1663-1671, doi: http://www.nature.com/onc/journal/v29/n11/suppinfo/onc2009447s1.html.
44. Chamorro MN, Schwartz DR, Vonica A, Brivanlou AH, Cho KR & Varmus HE (2005) FGF-20 and DKK1 are transcriptional targets of beta-catenin and FGF-20 is implicated in cancer and development. *EMBO J* **24**, 73-84, doi: 7600460 [pii] 10.1038/sj.emboj.7600460.
45. de Lau W, Peng WC, Gros P & Clevers H (2014) The R-spondin/Lgr5/Rnf43 module: regulator of Wnt signal strength. *Genes & Development* **28**, 305-316, doi: 10.1101/gad.235473.113.
46. Mao B, Wu W, Davidson G, Marhold J, Li M, Mechler BM, Delius H, Hoppe D, Stannek P, Walter C, et al. (2002) Kremen proteins are Dickkopf receptors that regulate Wnt/[beta]-catenin signalling. *Nature* **417**, 664-667.
47. Klipp E (2009) Timing matters. *FEBS Lett* **583**, 4013-4018, doi: http://dx.doi.org/10.1016/j.febslet.2009.11.065.
48. Heinrich R, Neel BG & Rapoport TA (2002) Mathematical models of protein kinase signal transduction. *Mol Cell* **9**, 957-970, doi: S1097276502005282 [pii].
49. Chen Y, Gruidl M, Remily-Wood E, Liu RZ, Eschrich S, Lloyd M, Nasir A, Bui MM, Huang E, Shibata D, et al. (2010) Quantification of beta-catenin signaling components in colon cancer cell lines, tissue sections, and microdissected tumor cells using reaction monitoring mass spectrometry. *J Proteome Res* **9**, 4215-4227.
50. Schwanhausser B, Busse D, Li N, Dittmar G, Schuchhardt J, Wolf J, Chen W & Selbach M (2011) Global quantification of mammalian gene expression control. *Nature* **473**, 337-342, doi: nature10098 [pii] 10.1038/nature10098.
51. Schwanhausser B, Busse D, Li N, Dittmar G, Schuchhardt J, Wolf J, Chen W & Selbach M (2013) Corrigendum: Global quantification of mammalian gene expression control. *Nature* **495**, 126-127.
52. Tan CW, Gardiner BS, Hirokawa Y, Layton MJ, Smith DW & Burgess AW (2012) Wnt signalling pathway parameters for mammalian cells. *PLoS One* **7**, e31882, doi: 10.1371/journal.pone.0031882 PONE-D-11-13188 [pii].
53. Tan CW, Gardiner BS, Hirokawa Y, Smith DW & Burgess AW (2014) Analysis of Wnt signaling beta-catenin spatial dynamics in HEK293T cells. *BMC Syst Biol* **8**, 44, doi: 10.1186/1752-0509-8-44

1752-0509-8-44 [pii].
54. Seki Y, Yamamoto H, Ngan CY, Yasui M, Tomita N, Kitani K, Takemasa I, Ikeda M, Sekimoto M, Matsuura N, et al. (2006) Construction of a novel DNA decoy that inhibits the oncogenic beta-catenin/T-cell factor pathway. *Mol Cancer Ther* **5**, 985-994, doi: 5/4/985 [pii] 10.1158/1535-7163.MCT-05-0388.
55. Gao C, Chen G, Romero G, Moschos S, Xu X & Hu J (2014) Induction of Gsk3β-β-TrCP Interaction Is Required for Late Phase Stabilization of β-Catenin in Canonical Wnt Signaling. *Journal of Biological Chemistry* **289**, 7099-7108, doi: 10.1074/jbc.M113.532606.
56. Ji N, Middelkoop Teije C, Mentink Remco A, Betist Marco C, Tonegawa S, Mooijman D, Korswagen Hendrik C & van Oudenaarden A (2013) Feedback Control of Gene Expression Variability in the Caenorhabditis elegans Wnt Pathway. *Cell* **155**, 869-880, doi: http://dx.doi.org/10.1016/j.cell.2013.09.060.
57. Tingzhe S, Ruoshi Y, Wei X, Feng Z & Pingping S (2010) Exploring a minimal two-component p53 model. *Phys Biol* **7**, 036008.
58. Harris SL & Levine AJ (2005) The p53 pathway: positive and negative feedback loops. **24**, 2899-2908.
59. Gonze D (2010) Coupling oscillations and switches in genetic networks. *Biosystems* **99**, 60-69, doi: http://dx.doi.org/10.1016/j.biosystems.2009.08.009.
60. Kim JR, Yoon Y & Cho KH (2008) Coupled feedback loops form dynamic motifs of cellular networks. *Biophys J* **94**, 359-365, doi: S0006-3495(08)70715-X [pii] 10.1529/biophysj.107.105106.
61. Pfeuty B & Kaneko K (2009) The combination of positive and negative feedback loops confers exquisite flexibility to biochemical switches. *Phys Biol* **6**, 046013, doi: 10.1088/1478-3975/6/4/046013.
62. Tyson JJ, Chen KC & Novak B (2003) Sniffers, buzzers, toggles and blinkers: dynamics of regulatory and signaling pathways in the cell. *Curr Opin Cell Biol* **15**, 221-231, doi: S0955067403000176 [pii].
63. Tsai TY, Choi YS, Ma W, Pomerening JR, Tang C & Ferrell JE, Jr. (2008) Robust, tunable biological oscillations from interlinked positive and negative feedback loops. *Science* **321**, 126-129, doi: 321/5885/126 [pii] 10.1126/science.1156951.
64. Anastas JN & Moon RT (2013) WNT signalling pathways as therapeutic targets in cancer. *Nat Rev Cancer* **13**, 11-26, doi: 10.1038/nrc3419.
65. Hart M, Concordet JP, Lassot I, Albert I, del los Santos R, Durand H, Perret C, Rubinfeld B, Margottin F, Benarous R, et al. (1999) The F-box protein beta-TrCP associates with phosphorylated beta-catenin and regulates its activity in the cell. *Curr Biol* **9**, 207-210, doi: S0960-9822(99)80091-8 [pii].
66. Ougolkov A, Zhang B, Yamashita K, Bilim V, Mai M, Fuchs SY & Minamoto T (2004) Associations among beta-TrCP, an E3 ubiquitin ligase receptor, beta-catenin, and NF-kappaB in colorectal cancer. *J Natl Cancer Inst* **96**, 1161-1170, doi: 10.1093/jnci/djh219 96/15/1161 [pii].
67. Heinrich R & Schuster S (1996) *The regulation of cellular systems*. Chapman & Hall, New York.
68. Kofahl B & Klipp E (2004) Modelling the dynamics of the yeast pheromone pathway. *Yeast* **21**, 831-850, doi: 10.1002/yea.1122.
69. Llorens M, Nuno JC, Rodriguez Y, Melendez-Hevia E & Montero F (1999) Generalization of the theory of transition times in metabolic pathways: a geometrical approach. *Biophys J* **77**, 23-36, doi: 10.1016/S0006-3495(99)76869-4.

70. Munemitsu S, Albert I, Souza B, Rubinfeld B & Polakis P (1995) Regulation of intracellular beta-catenin levels by the adenomatous polyposis coli (APC) tumor-suppressor protein. *Proc Natl Acad Sci U S A* **92**, 3046-3050.

Supporting information

Doc. S1: The HOS and FWD1 feedback model of Wnt/β-catenin signalling

includes:

a detailed description of the mathematical model, its equations and parameters, as well as

Fig. S1: Impact of different combinations of HOS and FWD1 feedback strengths on HOS, FWD1, and the β-catenin/TCF complex.

Fig. S2: Strong transcriptional up-regulation of FWD1 and/or HOS abolishes regulatory impact of the feedbacks on β-catenin/TCF dynamics.

Fig. S3: Impact of the FWD1 feedback strength on β-catenin/TCF steady state for different combinations of parameters k7r, k8r, and k17r.

Fig. S4: Impact of HOS and FWD1 feedback strength on the number and stability of β-catenin/TCF steady state.

Table S1: Parameter of the transient Wnt stimulus

Table S2: Kinetic parameters of the feedback model.

Table S3: Total protein concentrations of proteins obeying a conservation relation.

Table S4: Kinetic parameters to model mutations of APC.

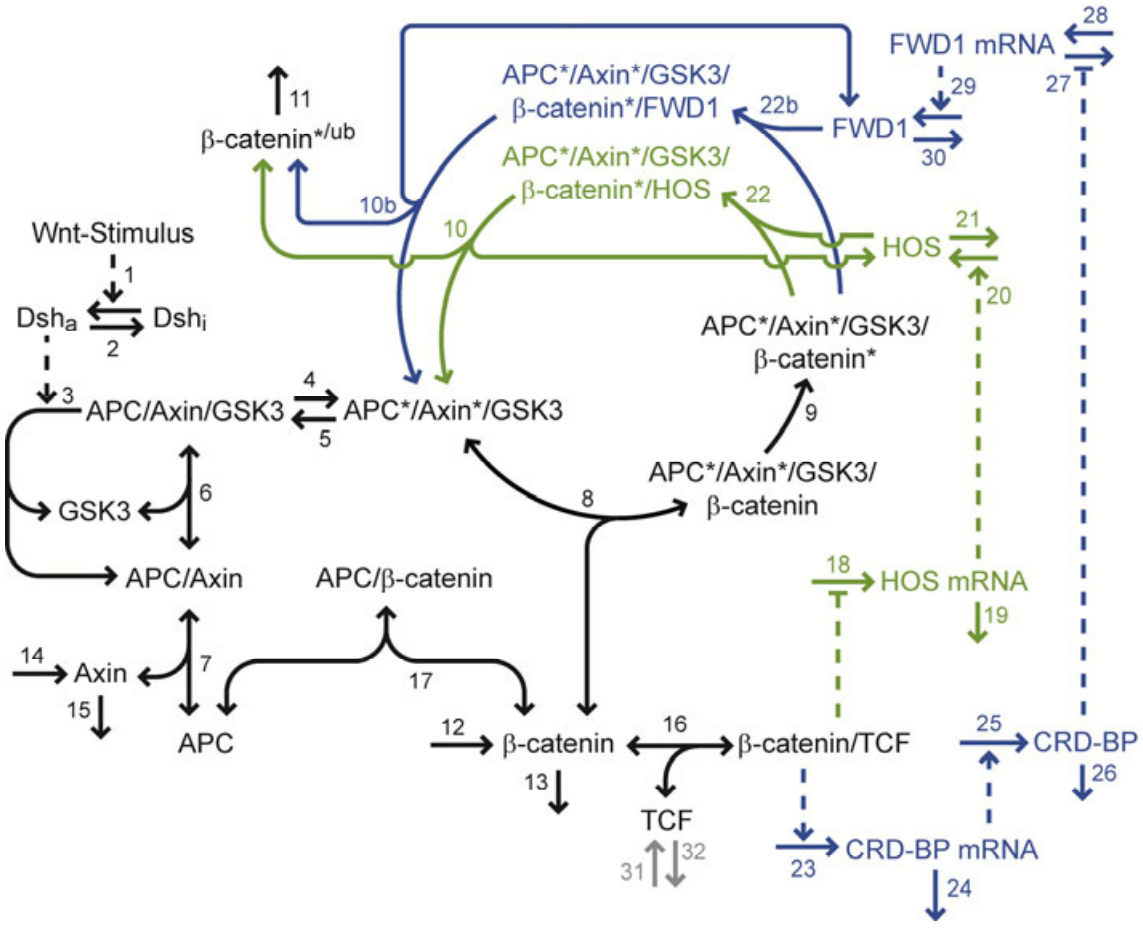

Figure 1: Reaction scheme of the Wnt/β-catenin pathway model that includes the FWD1 and HOS feedbacks.

The reaction scheme underlying the published model of Wnt/β-catenin signalling (black; reactions 1 - 9 and reactions 11 - 16) is extended by the HOS feedback (green; reactions 18 - 21) and FWD1 feedback (blue; reactions 23 - 30). HOS and FWD1 independently bind to the destruction complex to mediate the ubiquitination of phosphorylated β-catenin (reactions 10 and 22, and reactions 10b and 22b, respectively). The newly introduced TCF production and degradation are coloured in grey (reactions 31 and 32, respectively). One-headed arrows denote reactions taking place in the indicated direction. Double-headed arrows illustrate reversible binding reactions. Dashed arrows represent activation and dashed 'T's denote inhibition. Components in a complex are separated by a slash. The asterisk marks phosphorylation; ub stands for ubiquitinated species. The number next to an arrow specifies the number of the reaction. A detailed description of the model is provided in the supplementary Doc. S1.

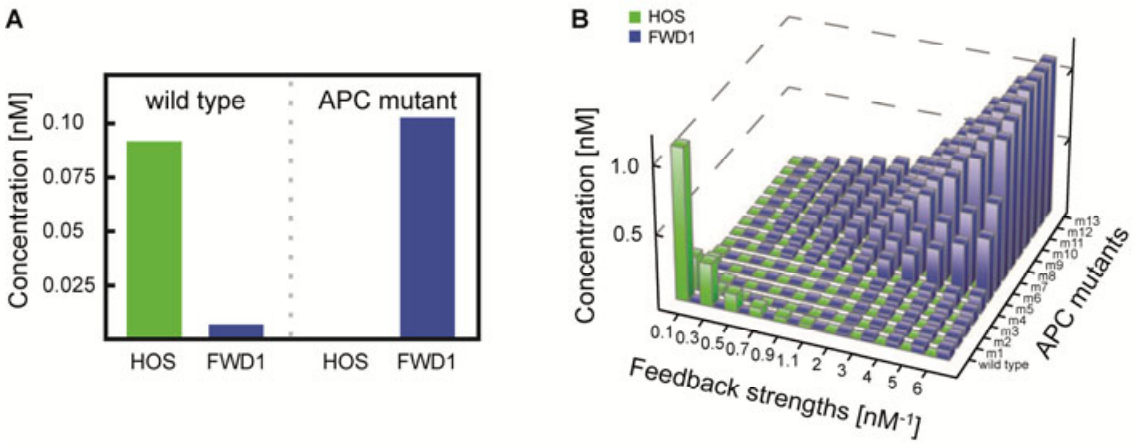

Figure 2: The feedback model reproduces the differential expression patterns of HOS and FWD1.

(A) Steady state concentrations of HOS (green bars) and FWD1 (blue bars) are calculated in the feedback model under wild type and APC mutant "m7" conditions (supplementary Doc. S1). HOS and FWD1 feedback strengths are both set to 0.6 nM^{-1} in the simulations. (B) Analysis shown in (A) is extended to HOS and FWD1 feedback strengths both set to identical values ranging from 0.1 nM^{-1} to 6 nM^{-1} considering APC mutant conditions "m1" to "m13".

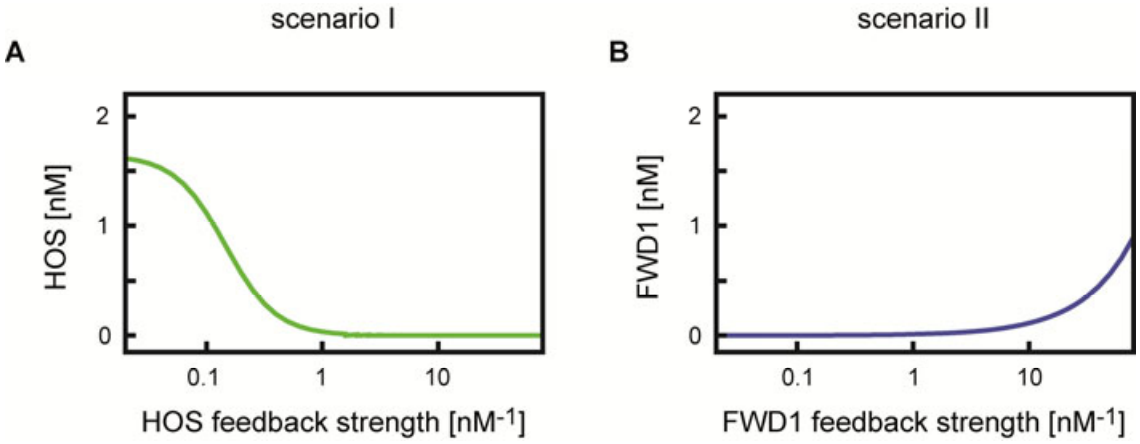

Figure 3: Variation of either HOS or FWD1 feedback strength allows for the independent modulation of HOS or FWD1 expression, respectively.

(A) HOS feedback strength is gradually increased while FWD1 feedback strength is set to zero (scenario I). The steady state concentration of HOS decreases due to increasing HOS feedback strength. (B) FWD1 feedback strength is gradually increased while HOS feedback strength is set to zero (scenario II). The steady state concentration of FWD1 rises due to increasing FWD1 feedback strength.

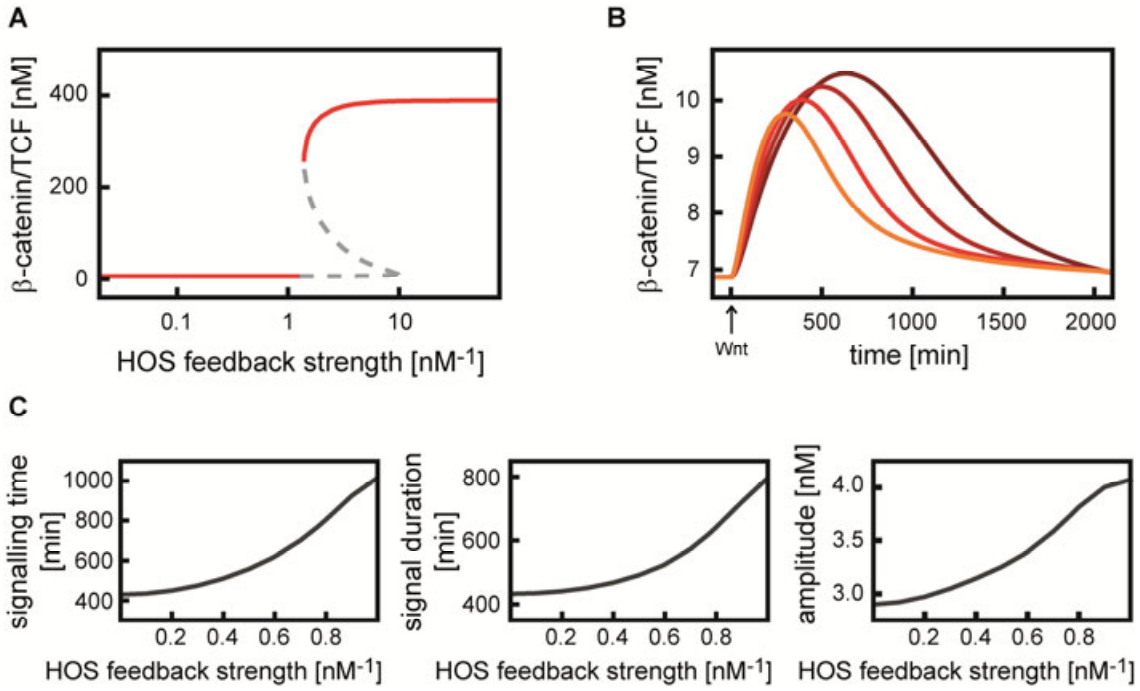

Figure 4: The HOS feedback affects β-catenin/TCF steady state and its dynamics upon Wnt stimulation.

(A) The steady state concentration of the β-catenin/TCF complex responds in a switch-like manner to increasing HOS feedback strength. The red lines denote stable steady state solutions; the grey dashed line marks unstable solutions. (B, C) Increasing HOS feedback strengths increase the signalling time, extend the signal duration, and increase the signal amplitude of β-catenin/TCF complex dynamics upon transient Wnt stimulation. The dynamics for different HOS feedback strengths are illustrated in (B): HOS feedback strength is set to zero (orange), 0.4 nM^{-1} (red), 0.6 nM^{-1} (darker red), and 0.8 nM^{-1} (dark red). Quantification of signalling time, signal duration, and signal amplitude of the dynamics for different HOS feedback strengths are shown in (C).

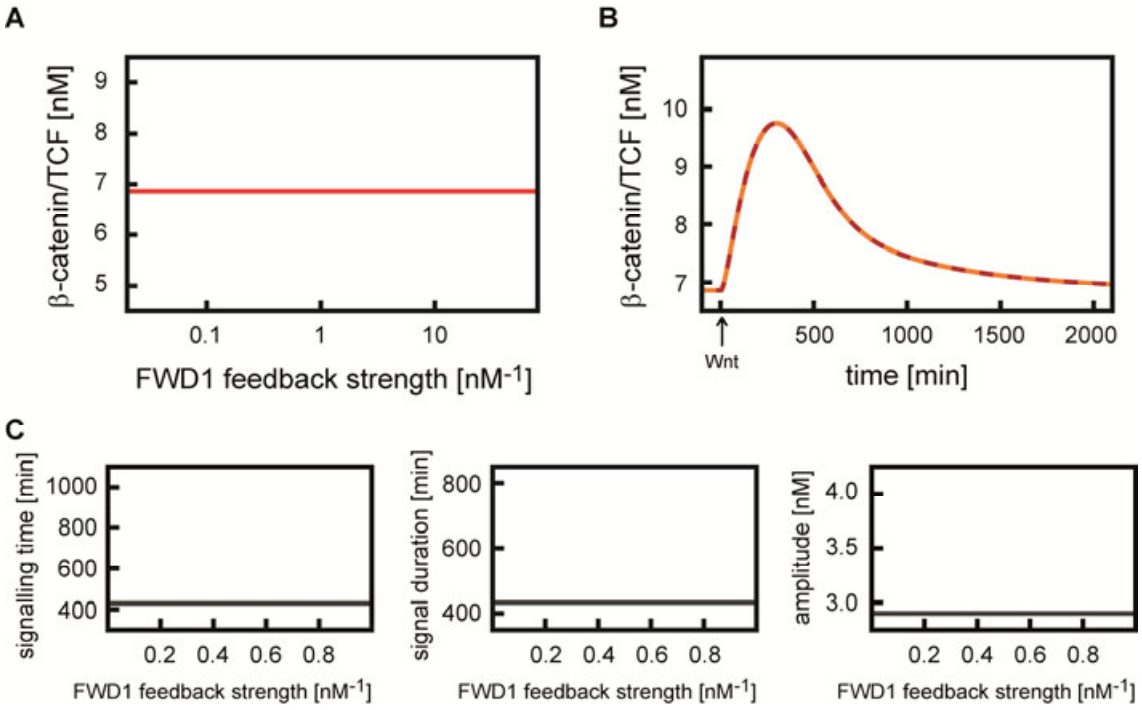

Figure 5: Changes in the FWD1 feedback strength do not affect β-catenin/TCF steady state concentration and dynamics in combination with a HOS feedback strength set to zero.

(A) The steady state concentration of β-catenin/TCF complex for different FWD1 feedback strengths. (B) Overlay of β-catenin/TCF complex dynamics upon transient Wnt stimulation comparing the FWD1 feedback strength set to zero (dashed orange) or set to 10 nM^{-1} (dashed dark red). (C) Quantification of signalling time, signal duration, and signal amplitude of the dynamics of the β-catenin/TCF complex for different values of the FWD1 feedback strength. The HOS feedback strength is set to zero in all simulations shown in this figure.

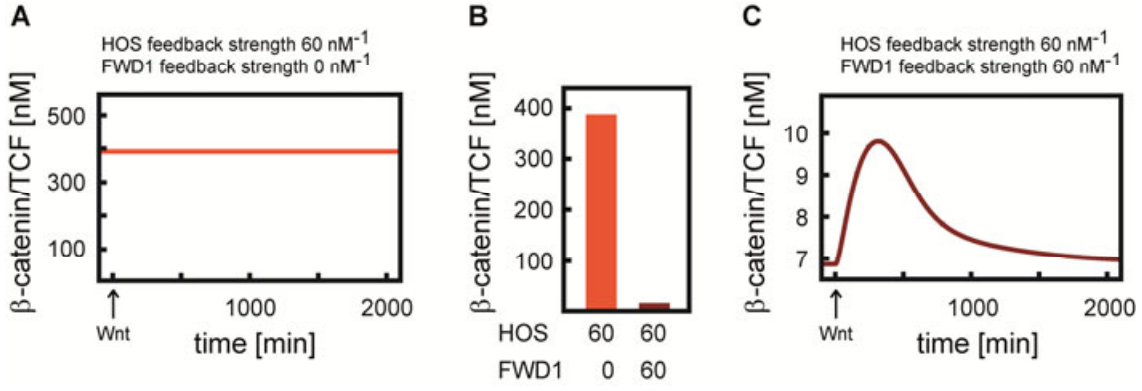

Figure 6: The FWD1 feedback influences the β-catenin/TCF steady state and its dynamics upon Wnt stimulation in combination with high HOS feedback strength.

A high HOS feedback strength (60 nM^{-1}) in combination with FWD1 feedback strength set to zero leads to a high the steady state concentration of the β-catenin/TCF complex (B, orange bar), which is maintained upon transient Wnt stimulation (A). In contrast, if both feedback strengths are set to 60 nM^{-1}, the steady state concentration of the β-catenin/TCF complex is low (B, dark red bar) and the β-catenin/TCF complex concentration transiently increases upon Wnt stimulation (C).

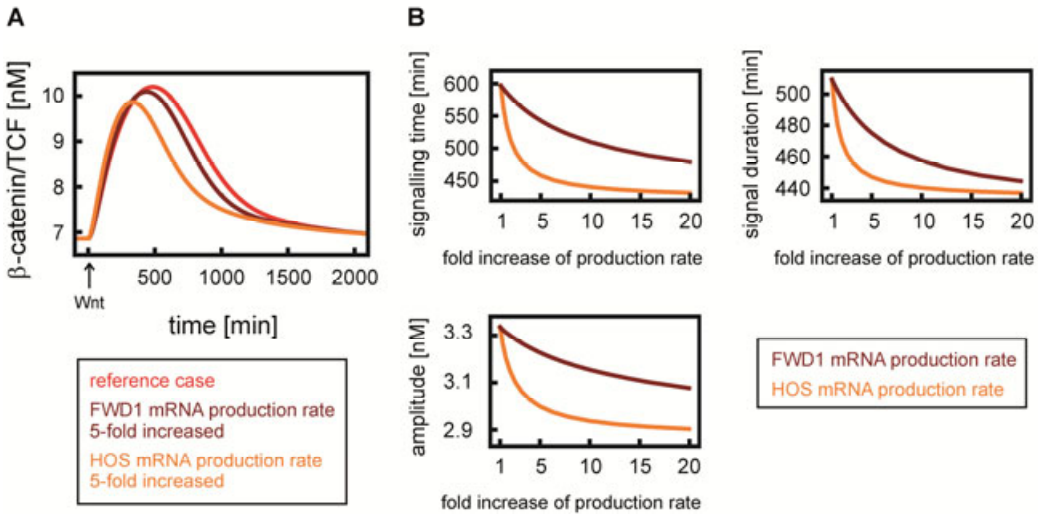

Figure 7: β-Catenin/TCF independent up-regulation of FWD1 or HOS concentration affects β-catenin/TCF dynamics upon Wnt stimulation.

(A) Different dynamics of the β-catenin/TCF complex upon transient Wnt stimulation for selected combinations of FWD1 and HOS mRNA production rates. Red: HOS and FWD1 production rates of 10^{-6} $nM \cdot min^{-1}$ (reference case); dark red: HOS and FWD1 production rates of 10^{-6} $nM \cdot min^{-1}$ and $5 \cdot 10^{-6}$ $nM \cdot min^{-1}$, respectively; orange: HOS and FWD1 production rates of $5 \cdot 10^{-6}$ $nM \cdot min^{-1}$ and 10^{-6} $nM \cdot min^{-1}$, respectively. (B) Quantification of signalling time, signalling duration, and signal amplitude of the dynamics of the β-catenin/TCF complex upon transient Wnt stimulation for different values of FWD1 mRNA production rate (dark red lines) or HOS mRNA production rate (orange lines). The HOS and FWD1 feedback strengths are both set to 0.6 nM^{-1} in all simulations.

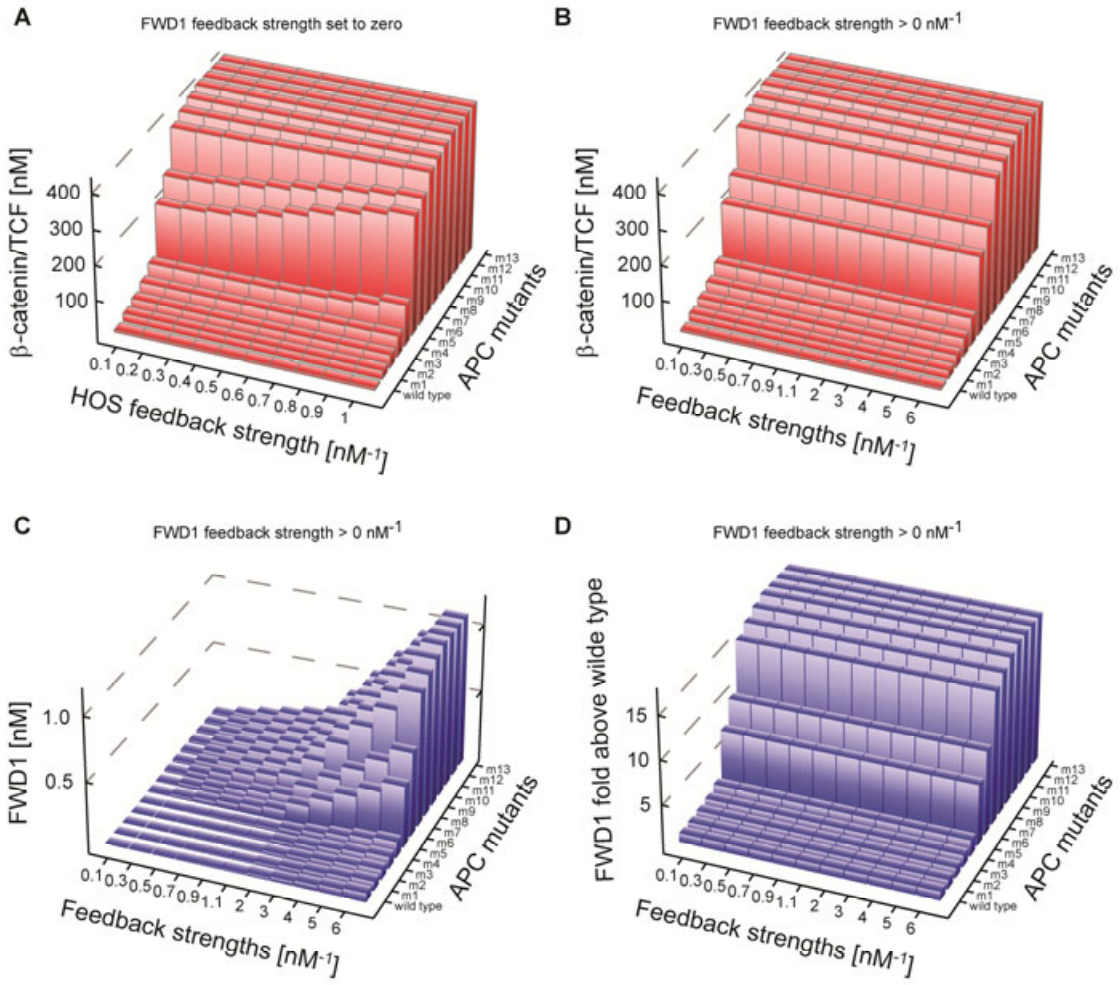

Figure 8: The FWD1 feedback mechanism does not protect against up-regulation of β-catenin/TCF concentrations induced by APC mutations.

(A) The steady state concentration of the β-catenin/TCF complex increases in APC truncation mutants "m1" to "m13" with respect to wild type conditions in the case of FWD1 feedback strength set to zero and HOS feedback strength ranging from 0.1 nM^{-1} to 1 nM^{-1}. (B) β-catenin/TCF steady state concentrations of wild type cells and APC mutants "m1" to "m13" for FWD1 and HOS feedback strengths both set to identical values ranging from 0.1 nM^{-1} to 6 nM^{-1}. (C) FWD1 steady state concentrations increase in APC mutants "m1" to "m13" with respect to wild type conditions. FWD1 and HOS feedback strengths are both set to identical feedback strengths ranging from 0.1 nM^{-1} to 6 nM^{-1}. (D) Fold increase of FWD1 steady state concentrations with respect to wild type is shown. This fold increase hardly changes for FWD1 and HOS feedback strengths set to identical values ranging from 0.1 nM^{-1} to 6 nM^{-1}. However, differences can be seen between wild type and APC mutants.

F

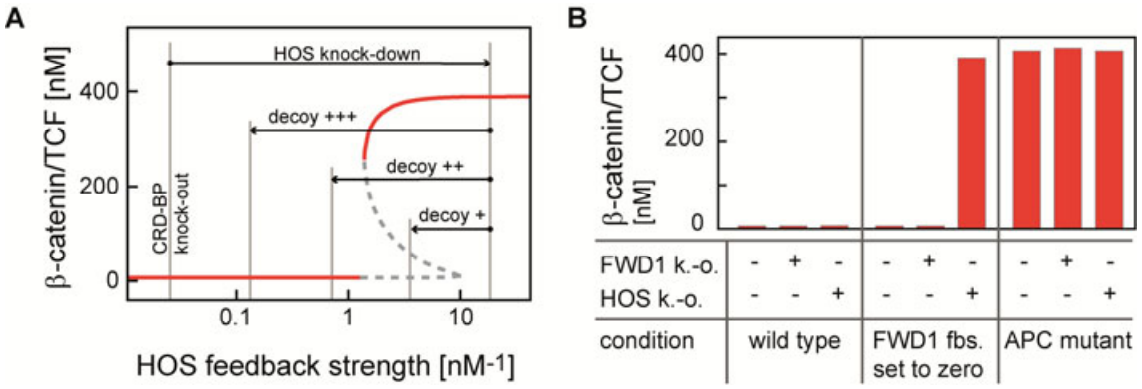

igure 9: Simulations of suggested experiments to validate model predictions.

(A) Proposed experimental setup to validate a switch-like response of β-catenin/TCF steady state concentrations upon changes in HOS feedback strength in combination with FWD1 feedback set to zero (Figure 4A). CRD-BP knock-out cells may represent the modelling scenario of FWD1 feedback set to zero. These cells contain low levels of β-catenin/TCF complex. Knock-down of HOS in CRD-BP knock-out cells will increase β-catenin/TCF complex concentrations. Application of increasing amounts of decoy oligonucleotides will reduce HOS feedback strength leading to a sudden switch-like reduction of β-catenin/TCF complex concentrations as predicted in Figure 4A. (B) Proposed experimental setup to test the different functions of the FWD1 and HOS feedback mechanisms. In wild type cells (bars 1-3), knock-out of FWD1 or HOS will not increase β-catenin/TCF steady state concentrations. Similarly, knock-out of FWD1 does not affect β-catenin/TCF concentrations in CRD-BP knock-out cells (bars 4 and 5). In contrast, knock-out of HOS strongly increases β-catenin/TCF concentrations in CRD-BP knock-out cells (bar 6). The model predicts that HOS and CRD-BP double knock-out (bar 6) increases β-catenin/TCF concentrations to similar extends as predicted under APC mutant “m9” conditions (bars 7-9). Corresponding example cell lines of APC mutant “m9” might be SW480 or SW620 cells, as they harbour truncations at codon 1338 [66]. Other cell lines representing APC mutants “m1” to “m8” may be constructed by transfecting truncated APC expression constructs in SW480 cells as has been previously described [43, 70]. 293T cells could potentially serve as “wild type” since to our knowledge no mutations of destruction complex components have been reported in this cell line.